

Nucleon strange quark content in $2 + 1$ -flavor QCD

**JLQCD collaboration: K. Takeda^{*a}, S. Aoki^{a,b}, S. Hashimoto^{c,d}, T. Kaneko^{c,d},
T. Onogi^e and N. Yamada^{c,d}**

^aGraduate School of Pure and Applied Sciences, University of Tsukuba, Tsukuba, Ibaraki
305-8571, Japan

^bCenter for computational Sciences, University of Tsukuba, Tsukuba, Ibaraki 305-8577, Japan

^cHigh Energy Accelerator Research Organization (KEK), Tsukuba 305-0801, Japan

^dSchool of High Energy Accelerator Science, The Graduate University for Advanced Studies
(Sokendai), Tsukuba 305-0801, Japan

^eDepartment of Physics, Osaka University Toyonaka, Osaka 560-0043, Japan

E-mail: ktakeda@het.ph.tsukuba.ac.jp

We calculate the strange quark content of the nucleon $\langle N | \bar{s}s | N \rangle$ directly from its disconnected three-point function in $N_f = 2 + 1$ QCD. Chiral symmetry is crucial to avoid a possibly large contamination due to operator mixing, and is exactly preserved by employing the overlap quark action. We also use the all-to-all quark propagator and the low-mode averaging technique in order to accurately calculate the relevant nucleon correlator. Our preliminary result extrapolated to the physical point is $f_{T_s} = m_s \langle N | \bar{s}s | N \rangle / M_N = 0.013(12)(16)$, where m_s and M_N are the masses of strange quark and nucleon. This is in good agreement with our previous estimate in $N_f = 2$ QCD as well as those from our indirect calculations using the Feynman-Hellmann theorem.

*The XXVIII International Symposium on Lattice Field Theory, Lattice2010
June 14-19, 2010
Villasimius, Italy*

^{*}Speaker.

1. Introduction

The strange quark content of the nucleon $\langle N|\bar{s}s|N\rangle$ is a fundamental quantity on the nucleon structure. It represents the effect of strange quark on the nucleon mass M_N

$$f_{T_s} = \frac{m_s \langle N|\bar{s}s|N\rangle}{M_N}, \quad (1.1)$$

where m_s is the strange quark mass. This parameter is also relevant to direct experimental searches for the dark matter, as one of its candidates, namely neutralino, may interact with the nucleon most strongly through the strange quark content. Therefore, $\langle N|\bar{s}s|N\rangle$ is crucial to assess the sensitivity of the experiments [1].

We calculate $\langle N|\bar{s}s|N\rangle$ from lattice QCD simulations in this study. The relevant nucleon three-point function is purely composed of a disconnected diagram, whose computational cost is prohibitively high with the conventional simulation methods. We overcome this difficulty by using the methods of the low-mode averaging [2, 3] and the all-to-all propagator [4].

Another advantage of our study is that chiral symmetry is exactly preserved by using the overlap quark action. We point out in this article that explicit symmetry breaking with conventional lattice fermions induces operator mixing leading to a possibly large contamination in $\langle N|\bar{s}s|N\rangle$.

2. Simulation setup

We simulate $N_f=2+1$ QCD with the Iwasaki gauge and the overlap quark actions. The lattice spacing is determined as $a = 0.112(1)$ fm using the Ω baryon mass as an input. We simulate two values of degenerate up and down quark masses $m_{ud} = 0.035$ and 0.050 on a $N_s^3 \times N_t = 16^3 \times 48$ lattice. The strange quark mass is set to $m_s = 0.080$ and 0.100 , which are close to the physical mass $m_{s,phys} = 0.081$ fixed from M_K . We also push our simulations to lighter masses $m_{ud} = 0.015$ and 0.025 on a larger lattice $24^3 \times 48$ but with a single value of $m_s = 0.080$. The four values of m_{ud} cover a range of $M_\pi \sim 290 - 520$ MeV with a condition $M_\pi L \gtrsim 4$ satisfied. We have accumulated about 50 independent gauge configurations at each combination of m_{ud} and m_s .

We calculate the nucleon three-point function

$$C_{3pt}^\Gamma(\mathbf{y}, t_{src}, \Delta t, \Delta t_s) = \frac{1}{N_s^6} \sum_{\mathbf{x}, \mathbf{z}} \left\{ \text{tr}_s \left[\Gamma \langle N(\mathbf{x}, t_{src} + \Delta t) \bar{s}s(\mathbf{z}, t_{src} + \Delta t_s) \bar{N}(\mathbf{y}, t_{src}) \rangle \right] - \langle \bar{s}s(\mathbf{z}, t_{src} + \Delta t_s) \rangle \text{tr}_s \left[\Gamma \langle N(\mathbf{x}, t_{src} + \Delta t) \bar{N}(\mathbf{y}, t_{src}) \rangle \right] \right\}, \quad (2.1)$$

where $N = \epsilon^{abc} (u_a^T C \gamma_5 d_b) u_c$ is the nucleon interpolating operator, and $\bar{s}s$ is the strange scalar operator on the lattice. We denote the temporal separation between the nucleon source and sink (scalar operator) by Δt (Δt_s). This correlator is calculated with four choices of the source location, namely $t_{src} = 0, 12, 24$ and 36 with $\mathbf{y} = 0$, and two choices of the projection operator $\Gamma = \Gamma_\pm = (1 \pm \gamma_4)/2$, which correspond to the forward and backward propagating nucleons. We then take the average

$$C_{3pt}(\Delta t, \Delta t_s) = \frac{1}{8} \sum_{t_{src}} \left\{ C_{3pt}^{\Gamma_+}(\mathbf{y}, t_{src}, \Delta t, \Delta t_s) + C_{3pt}^{\Gamma_-}(\mathbf{y}, N_t - t_{src}, N_t - \Delta t, N_t - \Delta t_s) \right\} \quad (2.2)$$

to reduce its statistical fluctuation. We also calculate the nucleon two-point function $C_{2pt}(\Delta t)$ in a similar way.

We calculate the disconnected strange quark loop from $\bar{s}s$ and its vacuum expectation value $\langle \bar{s}s \rangle$ using the all-to-all propagator. It is expected that low-lying modes of the Dirac operator D contribute dominantly to low-energy dynamics of QCD, and we calculate this contribution exactly

$$(D^{-1})_{low}(x, y) = \sum_{i=1}^{N_e} \frac{1}{\lambda^{(i)}} v^{(i)}(x) v^{(i)}(y)^\dagger \quad (Dv^{(i)} = \lambda^{(i)} v^{(i)}), \quad (2.3)$$

where the number of eigenmodes N_e is 160 (240) on our smaller (larger) lattice. The contribution of the remaining high-modes is estimated stochastically. We generate a single complex Z_2 noise vector $\eta(x)$ for each configuration, and divide it into $N_d = 3 \times 4 \times N_t/2$ vectors $\eta^{(d)}(x)$, which have non-zero elements only for a single combination of color and spinor indices on two consecutive time-slices. The high-mode contribution is then estimated as

$$(D^{-1})_{high}(x, y) = \sum_{d=1}^{N_d} \psi^{(d)}(x) \eta^{(d)}(y)^\dagger, \quad (2.4)$$

where $\psi^{(d)}(x)$ is obtained by solving

$$D\psi^{(d)}(x) = (1 - \mathcal{P}_{low})\eta^{(d)}(x), \quad \mathcal{P}_{low} = \sum_{i=1}^{N_e} v^{(i)}(x) v^{(i)}(y)^\dagger. \quad (2.5)$$

We note that, in this report, C_{3pt} on $24^3 \times 48$ is calculated without the high-mode contribution in the quark loop, our measurement of which is currently underway. In our study in $N_f = 2$ QCD [5, 6], we observed that the result for $\langle N | \bar{s}s | N \rangle$ is well dominated by the low-modes and does not change significantly by ignoring the high-mode contribution.

We can improve the statistical accuracy of the nucleon correlators by using LMA. Let us divide C_{2pt} into two contributions $C_{2pt,low}$ and $C_{2pt,high}$: $C_{2pt,low}$ is the two-point function constructed only from the low-mode part of the quark propagator $(D^{-1})_{low}$, and $C_{2pt,high}$ is the remaining contribution. We can average over all possible source points (\mathbf{y}, t_{src}) for $C_{2pt,low}$. The piece representing the nucleon propagation in C_{3pt} can be calculated in a similar way. In this study, we average over all t for t_{src} but 16 spatial locations for \mathbf{y} at each t_{src} .

In our previous study in $N_f = 2$ QCD, we observed that the smearing of the nucleon source and sink operators N is crucial to obtain a clear signal of C_{3pt} at reasonably small Δt . We therefore construct N from the quark field with the Gaussian smearing

$$q_{smr}(\mathbf{x}, t) = \sum_{\mathbf{y}} \left\{ \left(\mathbb{1} + \frac{\omega}{4N} H \right)^N \right\}_{\mathbf{x}, \mathbf{y}} q(\mathbf{y}, t), \quad H_{\mathbf{x}, \mathbf{y}} = \sum_{i=1}^3 (\delta_{\mathbf{x}, \mathbf{y}-\hat{i}} + \delta_{\mathbf{x}, \mathbf{y}+\hat{i}}), \quad (2.6)$$

where the parameters are set to $\omega = 20$ and $N = 400$. This smeared operator is not gauge invariant but we fix the gauge to the Coulomb gauge. We use q_{smr} for both C_{3pt} and C_{2pt} .

3. Strange quark content at simulated quark masses

We extract the strange quark content $\langle N | \bar{s}s | N \rangle$ on the lattice from the ratio of C_{3pt} and C_{2pt}

$$R(\Delta t, \Delta t_s) \equiv \frac{C_{3pt}(\Delta t, \Delta t_s)}{C_{2pt}(\Delta t)} \xrightarrow{\Delta t, \Delta t_s \rightarrow \infty} \langle N | \bar{s}s | N \rangle. \quad (3.1)$$

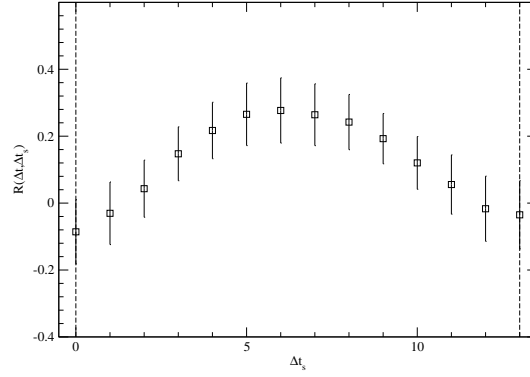


Figure 1: Ratio $R(\Delta t = 13, \Delta t_s)$ at $m_{ud} = 0.050$ and $m_s = 0.080$ as a function of Δt_s . The vertical lines show the locations of the nucleon operators. The noisy high-mode contribution to the quark loop is omitted in this plot.

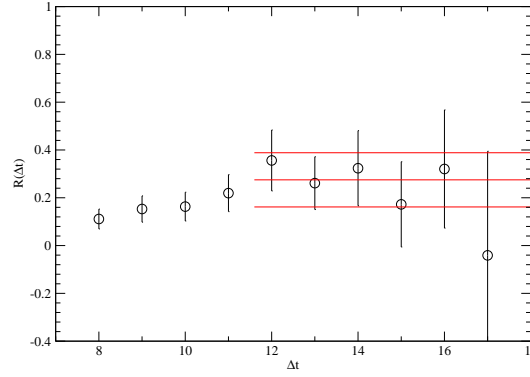


Figure 2: Fit result $R(\Delta t)$ at $m_{ud} = 0.050$ and $m_s = 0.080$ as a function of Δt . The horizontal lines show the result of a constant fit in Δt and its error band.

In order to identify a plateau of $R(\Delta t, \Delta t_s)$, it is helpful to consider the same ratio but approximated by taking only the low-mode contribution in the scalar loop. Figure 1 shows an example of the approximated ratio as a function of Δt_s . The significant change near $\Delta t_s \sim 0$ and Δt is due to a contamination from excited states. We therefore fit $R(\Delta t, \Delta t_s)$ to a constant form in $\Delta t_s = [5, \Delta t - 5]$, which is well separated from the nucleon source and sink. Note that this fit and the following analysis on $16^3 \times 48$ are carried out using $R(\Delta t, \Delta t_s)$ without the approximation. While we use the approximated ratio on $24^3 \times 48$ as mentioned in the previous section, we confirm in the analysis on $16^3 \times 48$ that the high-mode contribution to the quark loop has only small effect to $\langle N | \bar{s}s | N \rangle$.

The result of the constant fit in terms of Δt_s is denoted as $R(\Delta t)$ and is plotted as a function of Δt in Fig. 2. The stability of $R(\Delta t)$ at $\Delta t \geq 12$ suggests that these data are well dominated by the ground state contribution. We extract $\langle N | \bar{s}s | N \rangle$ by a constant fit to $R(\Delta t)$ in this region.

4. Chiral extrapolation to the physical point

In Fig. 3, we plot the matrix element $\langle N | \bar{s}s | N \rangle$ as a function of m_{ud} . Our data show a mild

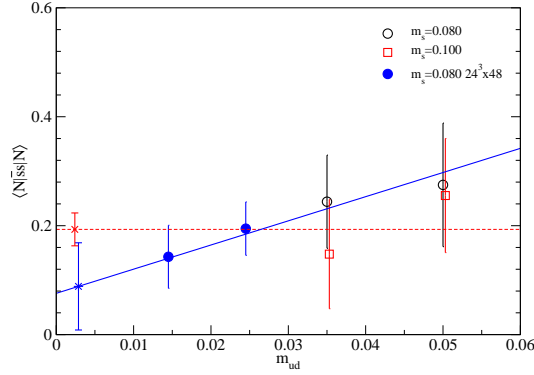


Figure 3: Strange quark content $\langle N|\bar{s}s|N \rangle$ as a function of m_{ud} . Circles and squares show data at $m_s = 0.080$ and 0.100 , whereas filled and open symbols are obtained on $16^3 \times 48$ and $24^3 \times 48$, respectively. We also plot the linear and constant fits by solid and dashed lines.

dependence on both m_{ud} and m_s , which can be well described by a linear form

$$\langle N|\bar{s}s|N \rangle = c_0 + c_{1,ud}m_{ud} + c_{1,s}m_s \quad (4.1)$$

with $\chi^2/\text{d.o.f.} \sim 0.06$. While we also attempt a chiral extrapolation based on heavy baryon chiral perturbation theory [7], the chiral expansion turns out to have a poor convergence up to the next-to-next-to-leading order at our simulated quark masses. We therefore use the linear chiral extrapolation. The systematic error due to the choice of the fitting form is estimated by comparing with a constant fit, which also leads to a reasonable value of $\chi^2/\text{d.o.f.} \sim 0.44$. We obtain $\langle N|\bar{s}s|N \rangle = 0.086(81)(107)$ at the physical point, where the first and second errors are statistical and systematic, respectively.

This bare matrix element is converted to the renormalization invariant parameter

$$f_{T_s} = \frac{m_s \langle N|\bar{s}s|N \rangle}{M_N} = 0.013(12)(16). \quad (4.2)$$

We note that this is in good agreement with our previous estimate in $N_f = 2$ QCD [5, 6] as well as our indirect determinations through the Feynman-Hellmann theorem in $N_f = 2$ [8] and $N_f = 2 + 1$ QCD [9].

5. Renormalization of $\bar{s}s$

In (4.2), f_{T_s} is expressed with the bare quantities assuming that the operator $m_s \bar{s}s$ is renormalization invariant as in the continuum limit. This is, however, not the case if chiral symmetry is explicitly broken by the lattice fermions of the choice. To illustrate this, let us consider the renormalization of the scalar operator $\bar{s}s$ in the flavor $SU(3)$ symmetric limit for simplicity. Using the flavor triplet quark field ψ , $\bar{s}s$ can be written as a linear combination of the flavor singlet and octet scalar operators

$$(\bar{s}s)^{phys} = \frac{1}{3} \left\{ (\bar{\psi}\psi)^{phys} - \sqrt{3} (\bar{\psi}\lambda^8\psi)^{phys} \right\}, \quad (5.1)$$

where λ^8 is a Gell-Mann matrix, and we put the superscript “*phys*” to the renormalized operators to distinguish them from bare lattice operators. The singlet and octet operators are renormalized as

$$(\bar{\psi}\psi)^{phys} = Z_0(\bar{\psi}\psi), \quad (5.2)$$

$$(\bar{\psi}\lambda^8\psi)^{phys} = Z_8(\bar{\psi}\lambda^8\psi), \quad (5.3)$$

in renormalization schemes which respect chiral symmetry. The operator $(\bar{s}s)^{phys}$ is thus expressed as

$$(\bar{s}s)^{phys} = \frac{1}{3} \{ (Z_0 + 2Z_8)(\bar{s}s) + (Z_0 - Z_8)(\bar{u}u + \bar{d}d) \}. \quad (5.4)$$

This implies that $\bar{s}s$ can mix with the up and down quark operators unless $Z_0 = Z_8$.

The difference $Z_0 - Z_8$ comes from disconnected diagrams, such as that in Fig. 4, contributing only to Z_0 . These diagrams are in fact forbidden by chiral symmetry: the quark loop with the scalar operator $\bar{s}s = \bar{s}_R s_L + \bar{s}_L s_R$ has to flip the chirality, while such a flip does not occur with the quark-quark-gluon vertices in the diagrams. This implies $Z_0 = Z_8$, which also holds at finite quark masses in mass independent renormalization schemes. The renormalization of $\bar{s}s$ thus reduces to a simple multiplicative renormalization

$$(\bar{s}s)^{phys} = Z_S \bar{s}s, \quad Z_S = Z_8 = Z_0, \quad (5.5)$$

and the operator $m_s \bar{s}s$ is renormalization invariant provided that chiral symmetry is exactly preserved as in our study.

When chiral symmetry is explicitly broken by a lattice fermion formulation, (5.5) is modified as

$$(\bar{s}s)^{phys} = \frac{1}{3} \left[(Z_0 + 2Z_8)(\bar{s}s)^{lat} + (Z_0 - Z_8)(\bar{u}u + \bar{d}d)^{lat} + \frac{b_0}{a^3} + \dots \right]. \quad (5.6)$$

The second term represents the mixing with the light quark contents due to $Z_0 \neq Z_8$. This may lead to a large contamination in $(\bar{s}s)^{phys}$, because the light quark contents induce a connected diagram, the magnitude of which is much larger than that of the disconnected one. Previous direct calculations with the Wilson-type fermions [10, 11, 12] in fact obtained rather large values $f_{T_s} \sim 0.3 - 0.5$ compared to our result (4.2) probably due to this contamination.

The explicit symmetry breaking also induces the mixing of the flavor-singlet operator $\bar{\psi}\psi$ with lower dimensional operators, such as the third term in (5.6), through the renormalization (5.2). This contribution must be subtracted as a part of the vacuum expectation value of $\bar{s}s$. Due to the cubic divergence, this results in a large cancellation, with which the calculation is potentially noisier.

6. Conclusion

We calculate the nucleon strange quark content in $N_f = 2 + 1$ QCD. Chiral symmetry is exactly preserved by employing the overlap quarks in order to avoid large contaminations from the operator mixing. We also use the LMA and the all-to-all propagator to accurately calculate the relevant nucleon correlators. Our result of f_{T_s} is in good agreement with our previous study in $N_f = 2$ QCD as well as our indirect calculations for $N_f = 2$ and 3 using the Feynman-Hellmann theorem: all our studies consistently favor small strange quark content $f_{T_s} \approx 0.02$.

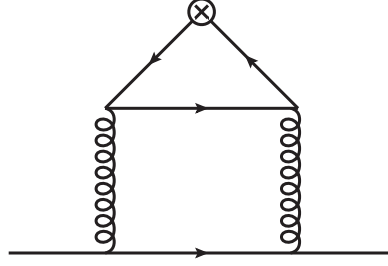


Figure 4: Disconnected diagram contributing the renormalization of the flavor singlet scalar operator (cross). In higher orders, more gluons propagate between the quark loop and propagator on the bottom.

Numerical simulations are performed on Hitachi SR11000 and IBM System Blue Gene Solution at High Energy Accelerator Research Organization (KEK) under a support of its Large Scale Simulation Program (No. 09/10-09). This work is supported in part by the Grant-in-Aid of the Ministry of Education, Culture, Sports, Science and Technology, (No. 20340047, 21674002 and 21684013) and by the Grant-in-Aid for Scientific Research on Innovative Areas, (No. 20105001, 20105002, 20105003 and 20105005).

References

- [1] J. R. Ellis, K. A. Olive and C. Savage, Phys. Rev. D **77**, 065026 (2008) [arXiv:0801.3656 [hep-ph]].
- [2] T. A. DeGrand and S. Schaefer, Comput. Phys. Commun. **159**, 185 (2004) [arXiv:hep-lat/0401011].
- [3] L. Giusti, P. Hernandez, M. Laine, P. Weisz and H. Wittig, JHEP **0404**, 013 (2004) [arXiv:hep-lat/0402002].
- [4] J. Foley, K. Jimmy Juge, A. O’Cais, M. Peardon, S. M. Ryan and J. I. Skullerud, Comput. Phys. Commun. **172**, 145 (2005) [arXiv:hep-lat/0505023].
- [5] K. Takeda *et al.* (JLQCD collaboration), PoS **LAT2009**, 141 (2009) [arXiv:0910.5036 [hep-lat]].
- [6] K. Takeda *et al.* (JLQCD collaboration), in preparation.
- [7] A. Walker-Loud, Nucl. Phys. A **747**, 476 (2005) [arXiv:hep-lat/0405007].
- [8] H. Ohki *et al.*, Phys. Rev. D **78**, 054502 (2008) [arXiv:0806.4744 [hep-lat]].
- [9] H. Ohki *et al.* (JLQCD collaboration), PoS **LAT2009**, 124 (2009) [arXiv:0910.3271 [hep-lat]].
- [10] M. Fukugita, Y. Kuramashi, M. Okawa and A. Ukawa, Phys. Rev. D **51**, 5319 (1995) [arXiv:hep-lat/9408002].
- [11] S.J. Dong, J.F. Lagae and K.F. Liu, Phys. Rev. D **54**, 5496 (1996) [arXiv:hep-ph/9602259].
- [12] S. Gusken *et al.* (T χ L Collaboration), Phys. Rev. D **59**, 054504 (1999) [arXiv:hep-lat/9809066].